AIAA JOURNAL
Vol. 51, No. 2, February 2013

External Mean Flow Effects on Noise Radiation from Orthogonally Rib-Stiffened Aeroelastic Plates

F. X. Xin* and T. J. Lu†
Xi'an Jiaotong University, Xi'an 710049, People's Republic of China

DOI: 10.2514/1.J051819

A theoretical modeling approach is proposed for noise radiated from aeroelastic skin plates of aircraft fuselage stiffened by orthogonally distributed rib-stiffeners and subjected to external jet-noise in the presence of mean flow. The focus is placed upon quantifying the effects of mean flow on the aeroelastic-acoustic characteristics of the rib-stiffened plate. The Euler–Bernoulli beam equation and the torsional wave equation governing separately the flexural and torsional motions of the rib-stiffeners are employed to accurately describe the force-moment coupling between the stiffeners and the plate. Given the periodicity of the structure, the resulting governing equations of the system are solved by applying the Poisson summation formula and the Fourier transformation technique. The radiated sound pressure is related to the plate displacement by means of the Helmholtz equation and the fluid-structure boundary conditions. To highlight the radiation characteristics of the periodically stiffened structure as well as the mean flow effects, the final radiated sound pressure is presented in the form of decibels with reference to that of a bare plate immersed in mean flow. Systematic parametric studies are conducted to evaluate the effects of external mean flow speed, noise incident angle and periodical spacings on the aeroelastic-acoustic performance of the rib-stiffened plate.

Nomenclature

c_0	=	sound speed in air
c_1	=	speed of sound in incident fluid medium
c_2	=	speed of sound in radiated fluid medium
D	=	flexural rigidity of aeroelastic panel
E	=	Young's modulus of panel material
E_x	=	Young's modulus of x-wise rib-stiffener material
E_y	=	Young's modulus of y-wise rib-stiffener material
G_x	=	shear modulus of the x-wise rib stiffener
G_y	=	shear modulus of the y-wise rib stiffener
H	=	height of rib stiffeners
h	=	thickness of face plate
I_x	=	the area moment of inertia around x axis
I_y	=	the area moment of inertia around y axis
I_{px}	=	polar moment of inertia for x-wise rib stiffener
I_{py}	=	polar moment of inertia for y-wise rib stiffener
J_x	=	polar moment of inertia for x-wise rib stiffener
J_y	=	polar moment of inertia for y-wise rib stiffener
k	=	sound wave number
k_x	=	wave number component in x direction
k_y	=	wave number component in y direction
k_z	=	wave number component in z direction
L_W	=	sound power level
l_x	=	periodic spacing between two adjacent y-wise rib stiffeners
l_y	=	periodic spacing between two adjacent x-wise rib stiffeners
M	=	Mach number
m	=	number of y-wise rib stiffeners
m_p	=	mass per unit area of face plate
m_x	=	surface mass of x-wise rib stiffener
m_y	=	surface mass of y-wise rib stiffener
M	=	dimension of matrix
m'	=	number of y-wise rib stiffeners
$\hat{m}$	=	truncated number of y-wise rib stiffeners
n	=	number of x-wise rib stiffeners
N	=	dimension of matrix
n'	=	number of x-wise rib stiffeners
$\hat{n}$	=	truncated number of x-wise rib stiffeners
p_e	=	amplitude of incident sound wave
P_i	=	incident sound pressure
$\tilde{P}_i$	=	Fourier transformation of incident sound pressure
P_r	=	reflected sound pressure
$\tilde{P}_r$	=	Fourier transformation of reflected sound pressure
P_t	=	transmitted (or radiated) sound pressure
$\tilde{P}_t$	=	Fourier transformation of transmitted (or radiated) sound pressure
P_{ts}	=	radiated sound pressure of rib-stiffened plate
$\tilde{P}_{ts}$	=	Fourier transformation of radiated sound pressure of rib-stiffened plate
P_{tu}	=	radiated sound pressure of bare plate
$\tilde{P}_{tu}$	=	Fourier transformation of radiated sound pressure of bare plate
$\boldsymbol{Q}$	=	general force matrix
q_s	=	force of y-wise rib stiffener
$\tilde{q}_s$	=	Fourier transformation for force of y-wise rib stiffener
q_t	=	force of x-wise rib stiffener
$\tilde{q}_t$	=	Fourier transformation for force of x-wise rib stiffener
$\boldsymbol{T}$	=	generalized stiffness matrix
t	=	time variable
t_x	=	thickness of x-wise rib stiffener
t_y	=	thickness of y-wise rib stiffener
$\boldsymbol{U}$	=	displacement matrix
$\boldsymbol{V}$	=	velocity vector of mean flow
v	=	speed of mean flow in x direction
w	=	flexural displacement of the plate
$W_{m'n'}$	=	amplitude of plate displacement
$\tilde{w}$	=	Fourier transformation of flexural displacement of face plate
α	=	wave number component in x direction
α_m	=	$\alpha_0 + 2m\pi/l_x$
α'_m	=	$\alpha_0 + 2m'\pi/l_x$
α_0	=	initial wavenumber component in x-direction
β	=	wave number component in y direction
β_n	=	$\beta_0 + 2n\pi/l_y$
β'_n	=	$\beta_0 + 2n'\pi/l_y$

Received 29 December 2011; revision received 30 August 2012; accepted for publication 4 September 2012; published online 10 December 2012.

*Faculty, State Key Laboratory for Mechanical Structure Strength and Vibration, School of Aerospace; fengxian.xin@gmail.com.

†Professor, State Key Laboratory for Mechanical Structure Strength and Vibration, School of Aerospace; tjlu@mail.xjtu.edu.cn.

β_0 = initial wave number component in y direction
γ_1 = $\gamma_1(\alpha,\beta) = \sqrt{\alpha^2+\beta^2-(\omega-v\alpha)^2/c_0^2}$
γ_2 = $\gamma_2(\alpha,\beta) = \sqrt{\alpha^2+\beta^2-\omega^2/c_0^2}$
Δ = $\{[D(\alpha^2+\beta^2)^2 - m\omega^2]\gamma_2(\alpha,\beta) - 2\omega^2\rho_0\}^{-1}$
$\delta(\cdot)$ = Dirac delta function
η = loss factor of panel material
θ = azimuth angle of mean flow
θ_x = $\partial w/\partial y$
θ_y = $\partial w/\partial x$
κ_s = moment of y-wise rib stiffener
$\tilde{\kappa}_s$ = Fourier transformation for moment of y-wise rib stiffener
κ_t = moment of x-wise rib stiffener
$\tilde{\kappa}_t$ = Fourier transformation for moment of x-wise rib stiffener
ν = Poisson ratio of panel material
$\prod_s$ = radiated sound power of rib-stiffened plate
$\prod_u$ = radiated sound power of bare plate
ρ_x = density of x-wise rib-stiffener material
ρ_y = density of y-wise rib-stiffener material
ρ_0 = density of air
ρ_1 = density of incident fluid medium
ρ_2 = density of radiation fluid medium
φ = elevation angle of incident sound wave
ω = circular frequency

I. Introduction

RECENT research and development in aircraft design have reconcentrated on the long-lasting concerns about external flow interaction with structure responses and noise radiation into the aircraft interior, which is of paramount importance for designing supersonic (or high subsonic) civil and military aircrafts with a lower interior noise level [1–19]. It has been widely regarded that the interior cabin noise is usually attributed to the direct incidence of engine exhaust noise and the high-speed turbulent boundary-layer (TBL) flow over the exterior fuselage [11–17,20–25], which generate a high level of noise, thereby affecting the comfort of passengers. In particular, the ultrahigh-bypass turbofans have remarkably increased tip Mach numbers, resulting in enhanced low-frequency noise impinging on the exterior of aircraft fuselages [3,26]. To reduce the cabin interior noise level, considerable efforts have been dedicated to addressing the increasingly pressing issue of external fluid-flow coupling with structure dynamic response.

Whereas early research on acoustic problems involving fluid flow concentrated on sound reflection and transmission at the idealized interface between a steady fluid medium and a moving fluid medium [27–29], numerous research studies in the past decades focused on the aeroelastic-acoustic interaction problem of an aeroelastic plate coupled with fluid flow. Concerning sound transmission through aircraft fuselage in the presence of external mean flow, Koval [2] derived a theoretical model for the field incidence transmission loss of a single-walled plate and calculated the effects of air flow, panel curvature, and internal fuselage pressurization. As an extension of Koval's model, Xin et al. [30] theoretically investigated the external mean flow effects on noise transmission through double-leaf plate structures. In this research, four different types of acoustic phenomena (namely, mass-air-mass resonance, standing-wave resonance, standing-wave attenuation, and coincidence resonance) for a planar double-leaf plate as well as the ring frequency resonance for a curved double-leaf plate were identified, with closed-form formulas for the natural frequencies of these phenomena derived based upon physical principles. To evaluate the influence of mean flow on boundary layer–generated interior noise, Howe and Shah [20] presented an analytical model to solve the acoustic radiation in terms of prescribed turbulent boundary-layer pressure fluctuation, which may be used to validate more general numerical schemes for fluid-structure interaction. With mean flow effects on forced vibroacoustic response of a baffled plate accounted for, Sgard et al. [31] proposed a coupled finite element method–boundary element method (FEM–BEM) approach to investigate the mean flow effects as well as the acoustic radiation pattern for a baffled plate with different kinds of boundary conditions; the mean flow effects were explicitly shown in terms of added mass, stiffness, and radiation damping. Considering the nonlinearities induced by in-plane forces and shearing forces due to the stretching of plate bending motion, Wu and Maestrello [32] developed theoretical formulations to estimate the dynamic and acoustic responses of a finite baffled plate subject to turbulent boundary-layer excitations. It was found that, in the presence of mean flow, the temporal instability can be induced by the added stiffness due to acoustic radiation, and the effect of added stiffness increased quadratically with mean flow speed. More recently, the effects of mean flow on sound transmission across a simply supported rectangular aeroelastic panel were analytically solved [33]. Focusing upon aircraft sidewall structures, Legault and Atalla [34,35] and Mejdi and Atalla [36] investigated theoretically the sound transmission problems of such periodically stiffened structures, and their theoretical predictions agreed well with experimental results.

In addition to the aforementioned investigations, various comprehensive studies [4,15,16,37–41] have been conducted on aeroelastic plates interacting with aerodynamic loading, including theoretical modeling for sound radiation and transmission as well as acoustic control scheme. In addition, to effectively reduce the interior noise level of aircraft cabin fuselages over a wide frequency range, various active strategies [11–13,21,26,42] were proposed to suppress the vibration and noise radiation of skin plates, providing alternative noise reduction solutions.

Although numerous experimental and theoretical studies concerning aeroelastic-acoustic problems of fuselage-like structures exist, at present, there lacks a thorough and fundamental understanding of the physical mechanism associated with the interaction between fluid flow and a vibrating structure. Specifically, although the factual construction of aircraft fuselage is commonly made of thin-walled structural elements with periodic rib stiffeners, the issue of aeroelastic-acoustic interaction for such structures has not been well addressed by existing studies. The focus of the present work is therefore placed upon the aeroelastic-acoustic problem of orthogonally rib-stiffened skin plates in the presence of external mean flow. A theoretical model is developed by combining the Kirchhoff thin-plate theory with the convected wave equation, with the fluid momentum equation applied to satisfy the fluid-structure boundary condition. The Euler–Bernoulli beam equation and the torsional wave equation are employed to describe the force-moment coupling between the rib stiffeners and the face plate. The system of governing equations is solved by applying the Poisson summation formula and Fourier transformation technique. Based on the theoretical formulations, systematic parametric studies are carried out to quantify how the external mean flow affects sound radiation from periodically stiffened aeroelastic plates and to explore the physical mechanisms underlying aeroelastic-acoustic interaction.

II. Theoretical Formulation

A. Dynamic Responses to Convected Harmonic Pressure

Typical aircraft fuselages are made of periodically rib stiffened plates and are often excited by external airflow and engine exhaust noise in cruise condition. To explore the dynamic response and sound radiation behavior of such rib-stiffened plates immersed in external airflow, a uniform plane sound wave varying harmonically in time is assumed to impinge on the plate from the external mean flow side, and the resulting sound radiation level within the interior static fluid side is examined. As shown in Fig. 1, the aeroelastic structure considered consists of a flat face sheet and two sets of orthogonally distributed rib stiffeners. Both the face sheet and the stiffeners are made of homogenous and isotropic materials, and the whole structure is immersed in inviscid, irrotational fluid media. The upper and bottom fluid media separated by the face plate occupy the spaces of $z < 0$ and $z > h$ and, in terms of mass density and sound speed, are characterized by (ρ_1, c_1) and (ρ_2, c_2), respectively. Let h denote the face plate thickness, H denote the height of the stiffeners, l_x and l_y denote the periodic spacings of the stiffeners in the x- and y-directions, and t_x and t_y denote the thicknesses of the stiffeners in the

x- and y-directions, respectively. The mean fluid flow with uniform speed v is assumed to move along the x direction. The incident sound wave transmitting from the external mean flow side is characterized by elevation angle φ_1 and azimuth angle θ with respect to the coordinate system defined in Fig. 1. The impinged noise excitation is partially reflected and partially transmitted through the structure via the face plate into the interior stationary fluid medium, which is strongly affected by the external mean flow and the rib stiffeners.

To analyze theoretically the system of Fig. 1, a number of simplifying assumptions are made: 1) the face plate is sufficiently thin so that it can be modeled using the classical Kirchhoff thin-plate theory; 2) the fluid media are taken as inviscid, irrotational, and incompressible [4–6,15,16,31,38–40,43]; and 3) the surface of the face plate adjacent to the mean flow is sufficiently smooth so that it is appropriate to consider the plate-fluid interface as one of the streamlines of the fluid flow, i.e., the mean flow is tangential to the acoustically deformed boundary [2,44].

With the forces and moments exerted by the rib stiffeners on the face plate accounted for, the normal displacement w of the plate is governed by

$$\begin{aligned} D\nabla^4 w + m_p \frac{\partial^2 w}{\partial t^2} &= -\sum_m q_s(x,y)\delta(x-ml_x) \\ &- \frac{\partial}{\partial x}\left[\sum_m \kappa_s(x,y)\delta(x-ml_x)\right] - \sum_n q_t(x,y)\delta(y-nl_y) \\ &- \frac{\partial}{\partial y}\left[\sum_n \kappa_t(x,y)\delta(y-nl_y)\right] \\ &+ P_i(x,y,0) + P_r(x,y,0) - P_t(x,y,h) \end{aligned} \tag{1}$$

where m_p is the surface mass; D is the flexural rigidity of the plate; q_s and κ_s are the forces and moments of y-wise stiffeners; q_t and κ_t are the forces and moments of x-wise stiffeners; P_i, P_r, and P_t are the incident, reflected, and radiated sound pressure; and m and n are the number of x- and y-wise stiffeners, respectively.

The Euler–Bernoulli beam equation and torsional wave equation governing the flexural and torsional motions of the rib stiffeners are shown in Eqs. (2) and (3) (note that the bending moments have been implicitly included in the Euler–Bernoulli equation, because the first-order partial derivative of the bending moments about the coordinate is equivalent to transverse force [45]):

1) x-wise stiffeners:

$$\begin{aligned} E_x I_x \frac{\partial^4 w}{\partial x^4} + m_x \frac{\partial^2 w}{\partial t^2} &= q_t(x,y), \\ G_x J_x \frac{\partial^2 \theta_x}{\partial x^2} - \rho_x I_{px} \frac{\partial^2 \theta_x}{\partial t^2} &= \kappa_t(x,y) \end{aligned} \tag{2}$$

2) y-wise stiffeners:

$$\begin{aligned} E_y I_y \frac{\partial^4 w}{\partial y^4} + m_y \frac{\partial^2 w}{\partial t^2} &= q_s(x,y), \\ G_y J_y \frac{\partial^2 \theta_y}{\partial y^2} - \rho_y I_{py} \frac{\partial^2 \theta_y}{\partial t^2} &= \kappa_s(x,y) \end{aligned} \tag{3}$$

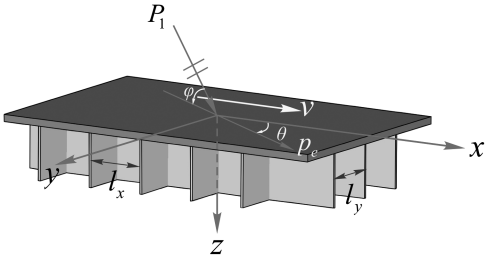

Fig. 1 Schematic of orthogonally rib-stiffened plate excited by convected harmonic pressure.

where $E_x I_x$, $G_x J_x$, I_{px}, ρ_x, and m_x are the flexural stiffness, torsional stiffness, polar moment of inertia, density, and surface mass for the x-wise stiffeners, respectively; $E_y I_y$, $G_y J_y$, I_{py}, ρ_y, and m_y are the flexural stiffness, torsional stiffness, polar moment of inertia, density, and surface mass for the y-wise stiffeners, respectively; and $\theta_x (= \partial_w/\partial_y)$ and $\theta_y (= \partial w/\partial x)$ are the torsion angles of the x- and y-wise stiffeners, respectively.

The incident sound pressure is taken as a traveling pressure wave excitation:

$$P_i(x,y,z) = p_e e^{i(\omega t - k_x x - k_y y - k_z z)} \tag{4}$$

where the sound wave number components depend upon the incident sound elevation angle φ and azimuth angle θ, as

$$k_x = k\cos\varphi\cos\theta, \qquad k_y = k\cos\varphi\sin\theta, \qquad k_z = k\sin\varphi \tag{5}$$

With k_x and k_y replaced by α_0 and β_0 as the initial wave number components, the incident sound pressure at the interface between air and plate can be written as

$$P_i(x,y,0) = p_e e^{i(\omega t - \alpha_0 x - \beta_0 y)} \tag{6}$$

The incident sound pressure in an inviscid and irrotational fluid moving in a plane parallel to the plate surface satisfies the convected wave equation [2,46], as

$$\frac{D^2 P_i}{Dt^2} = \left(\frac{\partial}{\partial t} + \mathbf{V}\cdot\nabla\right)^2 P_i = c_0^2 \nabla^2 P_i \tag{7}$$

When the uniform flow of velocity $\boldsymbol{V}$ moves along the x direction (Fig. 1), the wave equation for the mean flow is simplified as

$$\left(\frac{\partial}{\partial t} + v\cdot\frac{\partial}{\partial x}\right)^2 P_i = c_0^2 \nabla^2 P_i \tag{8}$$

Upon substituting Eq. (4) into Eq. (8), the wave number for the mean flow is obtained as

$$k = \frac{\omega}{c_0(1 + M\cos\varphi\cos\theta)} \tag{9}$$

where $M = v/c_0$ is the Mach number of the mean flow, and c_0 is the sound speed in fluid. When the fluid is stationary (i.e., $M = 0$), $k = \omega/c_0$.

Taking advantage of the periodicity of the rib-stiffened plates examined in the present study and employing the Poisson summation formula, we can express the wave components in the form of space harmonic series [47–52]:

$$\begin{aligned} \sum_m \delta(x - ml_x) &= \frac{1}{l_x}\sum_m e^{-i(2m\pi/l_x)x}, \\ \sum_n \delta(y - nl_y) &= \frac{1}{l_y}\sum_n e^{-i(2n\pi/l_y)y} \end{aligned} \tag{10}$$

The Fourier transformation pairs of a function with respect to (x, y) and (α, β) are defined as

$$w(x,y) = \int_{-\infty}^{+\infty}\int_{-\infty}^{+\infty} \tilde{w}(\alpha,\beta) e^{i(\alpha x + \beta y)}\,\mathrm{d}\alpha\mathrm{d}\beta \tag{11}$$

$$\tilde{w}(\alpha,\beta) = \left(\frac{1}{2\pi}\right)^2 \int_{-\infty}^{+\infty}\int_{-\infty}^{+\infty} w(x,y) e^{-i(\alpha x + \beta y)}\,\mathrm{d}x\mathrm{d}y \tag{12}$$

Applying the Poisson summation formula and taking the Fourier transformation of Eq. (1) leads to

$$
\begin{aligned}
&[D(\alpha^2+\beta^2)^2 - m\omega^2]\tilde{w}(\alpha,\beta)\\
&\quad = -\frac{1}{l_x}\sum_m[\tilde{q}_s(\alpha_m,\beta) + i\alpha\tilde{\kappa}_s(\alpha_m,\beta)]\\
&\quad -\frac{1}{l_y}\sum_n[\tilde{q}_t(\alpha,\beta_n) + i\beta\tilde{\kappa}_t(\alpha,\beta_n)]\\
&\quad + p_e\delta(\alpha+\alpha_0)\delta(\beta+\beta_0) + \tilde{P}_r(\alpha,\beta,0) - \tilde{P}_t(\alpha,\beta,h) \qquad (13)
\end{aligned}
$$

where $\alpha_m = \alpha + 2m\pi/l_x$; $\beta_n = \beta + 2m\pi/l_y$; and $\tilde{q}_s(\alpha_m,\beta)$, $\tilde{\kappa}_s(\alpha_m,\beta)$, $\tilde{q}_t(\alpha,\beta_n)$, and $\tilde{\kappa}_t(\alpha,\beta_n)$ can be obtained by taking the Fourier transformation of Eqs. (2) and (3):

$$\tilde{q}_s(\alpha_m,\beta) = [E_yI_y\beta^4 - m_y\omega^2]\tilde{w}(\alpha_m,\beta) \qquad (14)$$

$$\tilde{\kappa}_s(\alpha_m,\beta) = -[G_yJ_y\beta^2 - \rho_yI_{py}\omega^2](i\alpha_m)\tilde{w}(\alpha_m,\beta) \qquad (15)$$

$$\tilde{q}_t(\alpha,\beta_n) = [E_xI_x\alpha^4 - m_x\omega^2]\tilde{w}(\alpha,\beta_n) \qquad (16)$$

$$\tilde{\kappa}_t(\alpha,\beta_n) = -[G_xJ_x\alpha^2 - \rho_xI_{px}\omega^2](i\beta_n)\tilde{w}(\alpha,\beta_n) \qquad (17)$$

The sound pressure in incident side $P_i + P_r$ (including both the incident and reflected sound pressure) and the radiated sound pressure P_t satisfy the convected wave equation and the Helmholtz equation, respectively:

$$
\begin{aligned}
&\left(\frac{\partial^2}{\partial x^2}+\frac{\partial^2}{\partial y^2}+\frac{\partial^2}{\partial z^2}\right)[P_i(x,y,z)+P_r(x,y,z)]\\
&\quad -\frac{1}{c_0^2}\left(\frac{\partial}{\partial t}+v\cdot\frac{\partial}{\partial x}\right)^2[P_i(x,y,z)+P_r(x,y,z)] = 0 \qquad (18)
\end{aligned}
$$

$$\left(\frac{\partial^2}{\partial x^2}+\frac{\partial^2}{\partial y^2}+\frac{\partial^2}{\partial z^2}\right)P_t(x,y,z) + \left(\frac{\omega}{c_0}\right)^2 P_t(x,y,z) = 0 \qquad (19)$$

which, together with the boundary condition

$$\left.\frac{\partial(P_i+P_r)}{\partial z}\right|_{z=0} = \omega^2\rho_0 w, \qquad \left.\frac{\partial P_t}{\partial z}\right|_{z=h} = \omega^2\rho_0 w \qquad (20)$$

ensure the equality of fluid velocity at the fluid-solid interface and plate velocity, ρ_0 being the fluid density. Transforming Eqs. (18–20) yields

$$
\begin{aligned}
\tilde{P}_r(\alpha,\beta,z) &= p_e\delta(\alpha+\alpha_0)\delta(\beta+\beta_0)e^{\gamma_1 z}\\
&\quad + \omega^2\rho_0\tilde{w}(\alpha,\beta)e^{\gamma_1 z}/\gamma_1(\alpha,\beta) \qquad (21)
\end{aligned}
$$

$$\tilde{P}_t(\alpha,\beta,z) = -\omega^2\rho_0\tilde{w}(\alpha,\beta)e^{-\gamma_2 z+\gamma_2 h}/\gamma_2(\alpha,\beta) \qquad (22)$$

where

$$\gamma_1^2 = \alpha^2+\beta^2-(\omega-v\alpha)^2/c_0^2 \qquad (23)$$

$$\gamma_2^2 = \alpha^2+\beta^2-\omega^2/c_0^2 \qquad (24)$$

Incorporating Eqs. (14–17) and Eqs. (21) and (22) into Eq. (13) results in

$$
\begin{aligned}
&[D(\alpha^2+\beta^2)^2 - m\omega^2 - \omega^2\rho_0/\gamma_1(\alpha,\beta) - \omega^2\rho_0/\gamma_2(\alpha,\beta)]\tilde{w}(\alpha,\beta)\\
&\quad + \frac{1}{l_x}\sum_m[E_yI_y\beta^4 - m_y\omega^2 + \alpha\alpha_m(G_yJ_y\beta^2 - \rho_yI_{py}\omega^2)]\cdot\tilde{w}(\alpha_m,\beta)\\
&\quad + \frac{1}{l_y}\sum_n[E_xI_x\alpha^4 - m_x\omega^2 + \beta\beta_n(G_xJ_x\alpha^2 - \rho_xI_{px}\omega^2)]\cdot\tilde{w}(\alpha,\beta_n)\\
&\quad = 2p_e\delta(\alpha+\alpha_0)\delta(\beta+\beta_0) \qquad (25)
\end{aligned}
$$

To solve Eq. (25), (α,β) are replaced by (α'_m,β'_n), leading to a set of simultaneous algebraic equations:

$$
\begin{aligned}
&[D(\alpha_m'^2+\beta_n'^2)^2 - m\omega^2 - \omega^2\rho_0/\gamma_1(\alpha'_m,\beta'_n)\\
&\quad - \omega^2\rho_0/\gamma_2(\alpha'_m,\beta'_n)]\tilde{w}(\alpha'_m,\beta'_n)\\
&\quad + \frac{1}{l_x}\sum_m[E_yI_y\beta_n'^4 - m_y\omega^2 + \alpha'_m\alpha_m(G_yJ_y\beta_n'^2 - \rho_yI_{py}\omega^2)]\\
&\quad \cdot\tilde{w}(\alpha_m,\beta'_n)\\
&\quad + \frac{1}{l_y}\sum_n[E_xI_x\beta_m'^4 - m_x\omega^2 + \beta'_n\beta_n(G_xJ_x\alpha_m'^2 - \rho_xI_{px}\omega^2)]\\
&\quad \cdot\tilde{w}(\alpha'_m,\beta_n)\\
&\quad = 2p_e\delta(\alpha'_m+\alpha_0)\delta(\beta'_n+\beta_0) \qquad (26)
\end{aligned}
$$

To facilitate subsequent numerical calculations, this equation is rewritten as

$$
\begin{aligned}
&[D(\alpha_m'^2+\beta_n'^2)^2 - m\omega^2 - \omega^2\rho_0/\gamma_1(\alpha'_m,\beta'_n)\\
&\quad - \omega^2\rho_0/\gamma_2(\alpha'_m,\beta'_n)]\tilde{w}(\alpha'_m,\beta'_n)\\
&\quad + \frac{1}{l_x}(E_yI_y\beta_n'^4 - m_y\omega^2)\sum_m\tilde{w}(\alpha_m,\beta'_n)\\
&\quad + \frac{1}{l_x}\alpha'_m(G_yJ_y\beta_n'^2 - \rho_yI_{py}\omega^2)\sum_m\alpha_m\tilde{w}(\alpha_m,\beta'_n)\\
&\quad + \frac{1}{l_y}(E_xI_x\alpha_m'^4 - m_x\omega^2)\sum_n\tilde{w}(\alpha'_m,\beta_n)\\
&\quad + \frac{1}{l_y}\beta'_n(G_xJ_x\alpha_m'^2 - \rho_xI_{px}\omega^2)\sum_n\beta_n\tilde{w}(\alpha'_m,\beta_n)\\
&\quad = 2p_e\delta(\alpha'_m+\alpha_0)\delta(\beta'_n+\beta_0) \qquad (27)
\end{aligned}
$$

The amplitudes of the plate in the wave number space should satisfy an infinite set of simultaneous equations, which contain a doubly infinite number of unknowns: $\tilde{w}(\alpha'_m,\beta'_n)$ for $m' = -\infty,\infty$ and $n' = -\infty,\infty$. To perform numerical calculations, the equations can be truncated to retain a finite number of unknowns with $m' = -\hat{m},\hat{m}$ and $n' = -\hat{n},\hat{n}$ (insofar as the solutions converge). To be concise, the resulting simultaneous equations containing a finite number (i.e., MN, where $M = 2\hat{m}+1$ and $N = 2\hat{n}+1$) of unknowns can be expressed in matrix form as

$$\boldsymbol{T}_{MN\times MN}\boldsymbol{U}_{MN\times 1} = \boldsymbol{Q}_{MN\times 1} \qquad (28)$$

where $\boldsymbol{T}_{MN\times MN}$ denotes the generalized stiffness matrix, $\boldsymbol{U}_{MN\times 1}$ represents the displacement matrix, and $\boldsymbol{Q}_{MN\times 1}$ signifies the generalized force matrix. Detailed expressions for these matrices can be found in the Appendix. The resulting set of simultaneous equations for a total of MN unknowns is then numerically solved to obtain the solution for $\tilde{w}(\alpha,\beta)$.

B. Radiated Sound Pressure

As aforementioned, the displacement of the orthogonally rib-stiffened plate can be obtained by solving the governing equations:

$$\tilde{w}(\alpha,\beta)=\sum_{m'n'}W_{m'n'}\cdot 2p_e\delta(\alpha'_m+\alpha_0)\delta(\beta'_n+\beta_0) \tag{29}$$

where $W_{m'n'}$ is associated with the inverse form of the generalized stiffness matrix $\boldsymbol{T}_{MN\times MN}$. In fact, this expression gives the series form solution of Eq. (28).

Once the plate displacements are determined, the radiated sound pressure induced by plate vibration can be obtained by employing Eq. (22):

$$\tilde{P}_{\mathrm{ts}}(\alpha,\beta,h)=-\omega^2\rho_0\tilde{w}(\alpha,\beta)/\gamma_2(\alpha,\beta) \tag{30}$$

The radiated sound pressure in real physical space is calculated by applying the Fourier transformation:

$$\begin{aligned}P_{\mathrm{ts}}(x,y)&=\int_{-\infty}^{+\infty}\int_{-\infty}^{+\infty}\tilde{P}_{\mathrm{ts}}(\alpha,\beta)\cdot e^{i(\alpha x+\beta y)}\,\mathrm{d}\alpha\mathrm{d}\beta\\&=\int_{-\infty}^{+\infty}\int_{-\infty}^{+\infty}\sum_{m'n'}W_{m'n'}(-\omega^2\rho_0)\\&\cdot 2p_e\delta(\alpha'_m+\alpha_0)\delta(\beta'_n+\beta_0)/\gamma_2(\alpha,\beta)\cdot e^{i(\alpha x+\beta y)}\,\mathrm{d}\alpha\mathrm{d}\beta\\&=\sum_{m'n'}W_{m'n'}(-\omega^2\rho_0)\cdot 2p_e/\gamma_2\\&(-\alpha_0-2m'\pi/l_x,-\beta_0-2n'\pi/l_y)\cdot e^{-i[(\alpha_0+2m'\pi/l_x)x+(\beta_0+2n'\pi/l_y)y]}\end{aligned} \tag{31}$$

The truncation manipulation of Eq. (27) into a finite range actually implies that the infinite extent structure is replaced by a finite extent structure with geometrical dimensions of $Ml_x\times Nl_y$. It has been established that sufficiently large values chosen for M and N can ensure the solution convergence in subsequent numerical calculations. Correspondingly, the total radiated sound power can be evaluated by [10,40,53,54]

$$\begin{aligned}\prod_s&=\frac{1}{2}Re\left(\int_{-\hat{n}l_y}^{\hat{n}l_y}\int_{-\hat{m}l_x}^{\hat{m}l_x}P_{\mathrm{ts}}(x,y)\cdot v^*_{\mathrm{ts}}(x,y)\,\mathrm{d}x\mathrm{d}y\right)\\&=\frac{1}{2\rho_0c_0}\int_{-\hat{n}l_y}^{\hat{n}l_y}\int_{-\hat{m}l_x}^{\hat{m}l_x}\left|\sum\nolimits_{m'n'}W_{m'n'}(-\omega^2\rho_0)\cdot 2p_e/\gamma_2(\alpha_0+2m'\pi/^{\,l_x,\beta_0+2n'\pi/l_y)\cdot e^{-i[(\alpha_0+2m'\pi/l_x)x+(\beta_0+2n'\pi/l_y)y]}}\right|^2\mathrm{d}x\mathrm{d}y\\&=\frac{1}{2\rho_0c_0}\int_{-\hat{n}l_y}^{\hat{n}l_y}\int_{-\hat{m}l_x}^{\hat{m}l_x}\left|4\omega^4\rho_0^2p_e^2\sum_{mn,kl}\frac{W_{mn}W_{kl}}{\gamma_2(\alpha_m,\beta_n)\gamma_2(\alpha_k,\beta_l)}\cdot e^{-i(\alpha_mx+\beta_ny)}e^{-i(\alpha_kx+\beta_ly)}\right|\mathrm{d}x\mathrm{d}y\\&=\frac{2}{\rho_0c_0}\omega^4\rho_0^2p_e^2\left|\sum_{mn,kl}\frac{W_{mn}W_{kl}}{\gamma_2(\alpha_m,\beta_n)\gamma_2(\alpha_k,\beta_l)}\cdot\frac{4}{(\alpha_m+\alpha_k)(\beta_n+\beta_l)}\cdot\sin[(\alpha_m+\alpha_k)\hat{m}l_x]\sin[(\beta_n+\beta_l)\hat{n}l_y]\right|\end{aligned} \tag{32}$$

where the symbol $*$ denotes a complex conjugate, and $v_{\mathrm{ts}}(x,y)=P_{\mathrm{ts}}(x,y)/(\rho_0c_0)$ is the local acoustic velocity on the condition of plane waves assumption.

To highlight the radiation characteristics of periodically rib-stiffened structures as well as the mean flow effects, the solution for a bare face plate without any rib stiffeners in steady fluid is given in Eq. (37), which is also used as a reference. The displacement of a bare plate can be easily obtained from Eq. (25) by disregarding the terms related to the rib stiffeners:

$$\tilde{w}(\alpha,\beta)=\frac{2p_e\delta(\alpha+\alpha_0)\delta(\beta+\beta_0)}{D(\alpha^2+\beta^2)^2-m\omega^2-2\omega^2\rho_0/\gamma_2(\alpha,\beta)} \tag{33}$$

The radiated sound pressure is

$$\tilde{P}_{\mathrm{tu}}(\alpha,\beta,h)=-\omega^2\rho_0\tilde{w}(\alpha,\beta)/\gamma_2(\alpha,\beta) \tag{34}$$

Incorporating Eq. (33) and taking the Fourier transformation of Eq. (34) yields

$$\begin{aligned}P_{\mathrm{tu}}(x,y)&=\int_{-\infty}^{+\infty}\int_{-\infty}^{+\infty}\tilde{P}_{\mathrm{tu}}(\alpha,\beta)\cdot e^{i(\alpha x+\beta y)}\,\mathrm{d}\alpha\mathrm{d}\beta\\&=\int_{-\infty}^{+\infty}\int_{-\infty}^{+\infty}\Delta(\alpha,\beta)(-\omega^2\rho_0)\\&\cdot 2p_e\delta(\alpha+\alpha_0)\delta(\beta+\beta_0)e^{i(\alpha x+\beta y)}\,\mathrm{d}\alpha\mathrm{d}\beta\\&=\Delta(-\alpha_0,-\beta_0)(-\omega^2\rho_0)\cdot 2p_e e^{-i(\alpha_0x+\beta_0y)}\end{aligned} \tag{35}$$

where

$$\begin{aligned}\Delta(\alpha,\beta)&=\{[D(\alpha^2+\beta^2)^2-m\omega^2]\gamma_2(\alpha,\beta)-2\omega^2\rho_0\}^{-1},\\\gamma_2(\alpha,\beta)&=\sqrt{\alpha^2+\beta^2-\omega^2/c_0^2}\end{aligned} \tag{36}$$

The total radiated sound power by a bare plate having the same geometrical dimensions as the rib-stiffened plate is [10,40,53,54]

$$\begin{aligned}\prod_u&=\frac{1}{2}Re\left(\int_{-\hat{n}l_y}^{\hat{n}l_y}\int_{-\hat{m}l_x}^{\hat{m}l_x}P_{\mathrm{tu}}(x,y)\cdot v^*_{\mathrm{tu}}(x,y)\,\mathrm{d}x\mathrm{d}y\right)\\&=\frac{1}{2\rho_0c_0}\int_{-\hat{n}l_y}^{\hat{n}l_y}\int_{-\hat{m}l_x}^{\hat{m}l_x}\left|\Delta(\alpha_0,\beta_0)(-\omega^2\rho_0)\cdot 2p_e e^{-i(\alpha_0x+\beta_0y)}\right|^2\mathrm{d}x\mathrm{d}y\\&=\frac{2}{\rho_0c_0}\omega^4\rho_0^2p_e^2\int_{-\hat{n}l_y}^{\hat{n}l_y}\int_{-\hat{m}l_x}^{\hat{m}l_x}\left|\Delta^2(\alpha_0,\beta_0)e^{-2i(\alpha_0x+\beta_0y)}\right|\mathrm{d}x\mathrm{d}y\\&=\frac{2}{\rho_0c_0}\omega^4\rho_0^2p_e^2\left|\frac{\sin(2\alpha_0\hat{m}l_x)\sin(2\beta_0\hat{n}l_y)}{\alpha_0\beta_0\{[D(\alpha_0^2+\beta_0^2)^2-m\omega^2]\gamma_2(\alpha_0,\beta_0)-2\omega^2\rho_0\}^2}\right|\end{aligned} \tag{37}$$

where the symbol $*$ denotes a complex conjugate, and $v_{\mathrm{tu}}(x,y)=P_{\mathrm{tu}}(x,y)/(\rho_0c_0)$ is the local acoustic velocity on the condition of plane waves assumption.

Finally, with the bare plate taken as a reference, the radiated sound power level (PWL) L_{W} of the orthogonally rib-stiffened plate is expressed in decibel scale as

$$L_{\mathrm{W}}=10\log_{10}\left(\frac{\prod_s}{\prod_u}\right) \tag{38}$$

The sound PWL L_{W} thus defined is applied in the following section to quantify how the external mean flow affects the process of noise transmission and reveal the underlying physical mechanisms.

III. Parametric Study for Structural Sound Radiation

The aeroelastic-acoustic model and solution procedure presented in the preceding section are used to investigate the influence of

external mean flow on the transmission of jet-engine noise through rib-stiffened aircraft fuselage into an aircraft interior. To provide a comprehensive parametric study, the effects of Mach number, noise incident angle, and periodic spacings of the rib stiffeners on structural sound radiation are quantified.

For numerical calculations, the physical parameters and structural dimensions of the system are taken as follows. The face plate and rib stiffeners are both made of aluminum alloy with Young's modulus $E = 70$ GPa, Poisson ratio $\nu = 0.33$, and loss factor $\eta = 0.01$, typical for skin panel material of commercial aircrafts. The face plate has thickness $h = 0.002$ m, whereas the rib stiffeners have thickness $t_x = t_y = 0.001$ m and height $H = 0.08$ m. The fluid media surrounding the structure (see Fig. 1) are taken as air, with density $\rho_1 = \rho_2 = 1.21$ kg/m^3 and sound speed $c_1 = c_2 = 343$ m/s.

A. Effect of Mach Number

Given that the primary objective of this investigation is to examine how external mean flow affects noise transmission through a rib-stiffened aeroelastic plate into an aircraft interior, the Mach number as a key parameter for external mean flow falls into the focal point category. To highlight the periodicity of the stiffened plate as well as the external mean flow effects, the radiated sound power of the structure immersed in mean flow is normalized by that of the bare face plate in stationary fluid, i.e., Eq. (38). Figure 2 plots the predicted structure radiated sound pressure as a function of frequency for selected Mach numbers (i.e., $M = 0$, 0.4, 0.8, and 1.2), with $\varphi = 60\times$ deg, $\theta = 0$ deg, and $l_x = l_y = 0.2$ m.

It is seen from Fig. 2 that the presence of external mean flow significantly affects sound radiated from the rib-stiffened plate, as evidenced by the dramatic difference between the overall tendency of sound PWL L_W versus the frequency curve for case $M = 0$ and that for other cases ($M = 0.4$, 0.8, and 1.2). The curves associated with mean flow exhibit a similar tendency, although the specific PWL values and peak (or dip) locations differ for different Mach numbers. The results of Fig. 2 show that the presence of mean flow visually reduces the PWL at low frequencies (<80 Hz) and enhances the modal behavior of the periodically rib-stiffened plate. Further, as the Mach number is increased, whereas the PWL decreases at low frequencies (<80 Hz), the location of the corresponding resonance peak remains approximately unchanged while the antiresonance dips move to higher frequencies. These results imply the substantial influence of structural periodicity and external mean flow on sound radiation from rib-stiffened plates immersed in mean flow, because the choice of dimensionless PWL (with reference to that of a bare plate) eliminates other system factors.

To explore more details associated with the sound radiation properties of rib-stiffened plates in the presence of external mean flow, Fig. 3 presents the sound PWL in decibels with reference to 10^{-12} W of the rib-stiffened plate and the reference sound PWL in dB with reference to 10^{-12} W radiated from a bare plate under harmonic plane sound wave excitation of 1 Pa pressure. It is seen from Fig. 3 that the presence of mean flow leads to a modest decrease in the radiated sound power of the structure, thereby increasing the sound transmission loss. This feature is consistent with the existing results of Koval [2]. Moreover, as the Mach number is increased, the overall radiated sound power of the structure decreases, especially in the low frequency range. Also, with the increase of the Mach number, the modal dips appearing in the PWL curve shift to higher frequencies, which implies that the presence of mean flow increases the modal frequency of the structure. If one notes that the location of the first dip in the PWL versus the frequency curve of the stiffened plate at $M = 0$ is coincident with that of the first dip in the PWL curve of the bare plate at $M = 0$, it is understandable that no peak will appear at this location in the PWL curve of the stiffened plate at $M = 0$ due to the counteraction between the two. In contrast, while the first dips in the PWL curve of the stiffened plate at $M \neq 0$ move to higher frequencies, a peak will appear at this location in the PWL curve of the stiffened plate at $M \neq 0$.

B. Effect of Incidence Angle

For an aircraft in cruise condition, the noise induced by jet-engine or screw propeller may impact the fuselage skin structure at different incidence angles, depending upon the cruise speed and the skin structure location with respect to the source of the noise. Therefore, the effect of the noise incidence angle on sound radiation has actual significance in the evaluation of aircraft interior noise at different cruise speeds as well as the design of specific skin structures. Figure 4 plots the radiated sound PWL as a function of frequency for varying incidence angles, with $\theta = 0$ deg, $M = 0.8$ (selected for typical aircraft cruise speed; the following cases are also choose $M = 0.8$), and $l_x = l_y = 0.2$ m. A notable feature of Fig. 4 is that the peaks and dips in the PWL versus frequency curves shift to higher frequencies as the incidence angle is increased. Correspondingly, this induces changes in sound PWL at specific frequencies and the resultant alteration of the whole curve tendency. The sound wave with a more oblique sound incidence angle (i.e., a smaller incidence angle φ in the present coordinate of Fig. 1) is capable of exciting flexural bending waves with more frequency components in the plate, which is thus more likely to induce modal resonance and antiresonance over a wider frequency range. As a result, the peaks and dips move to lower frequencies as the incidence angle is decreased, as shown in Fig. 4.

In the presence of mean flow with Mach number $M = 0.8$, Fig. 5 presents both the PWL of the rib-stiffened plate and the reference PWL of the bare plate, in dB with reference to 10^{-12} W. As the sound incidence angle is increased, the dips in the PWL curves of both the bare plate and the rib-stiffened plate shift to higher frequencies. Moreover, the PWL values decrease with increasing sound incidence angle in a wide frequency range, which is particularly significant in

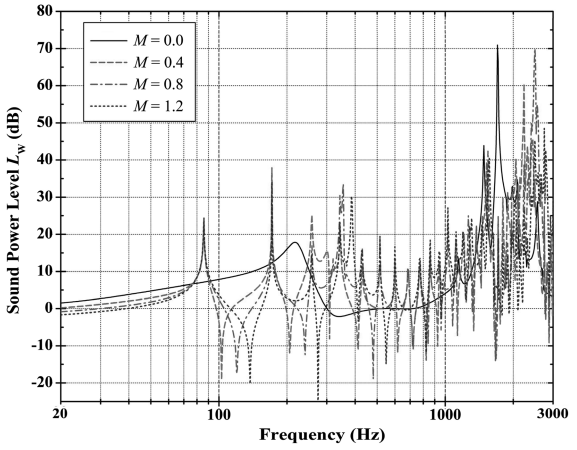

Fig. 2 Radiated sound power of the rib-stiffened plate (with reference to that of the bare plate) plotted as a function of frequency for selected Mach numbers of mean flow ($\varphi = 60$ deg, $\theta = 0$ deg, $l_x = l_y = 0.2$ m).

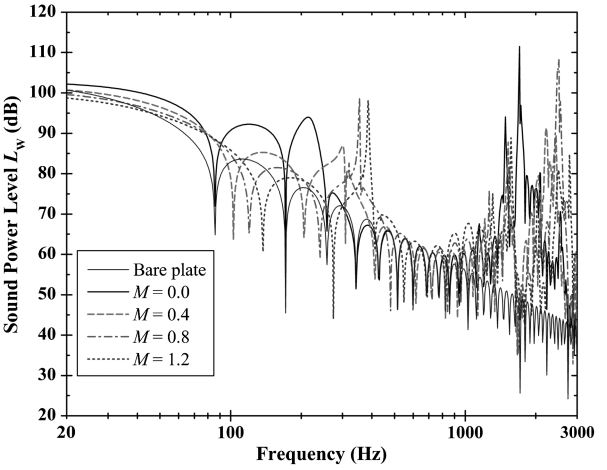

Fig. 3 Radiated sound power of the bare plate and the rib-stiffened plate (with reference to 10^{-12} W) plotted as a function of frequency for selected Mach numbers of mean flow ($\varphi = 60$ deg, $\theta = 0$ deg, $l_x = l_y = 0.2$ m).

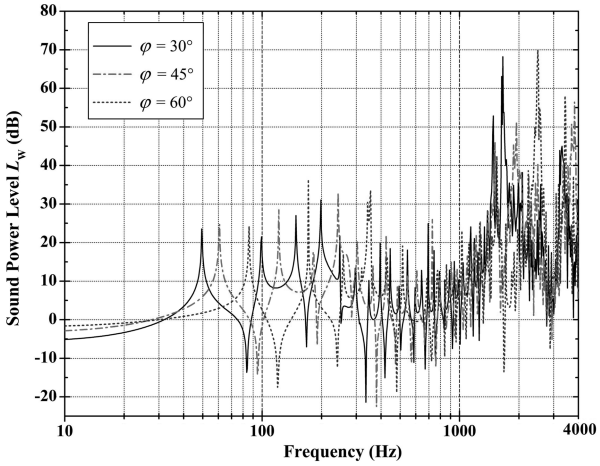

Fig. 4 Radiated sound power of the rib-stiffened plate (with reference to that of the bare plate) plotted as a function of frequency for various incident angles ($\theta = 0$ deg, $M = 0.8$, $l_x = l_y = 0.2$ m).

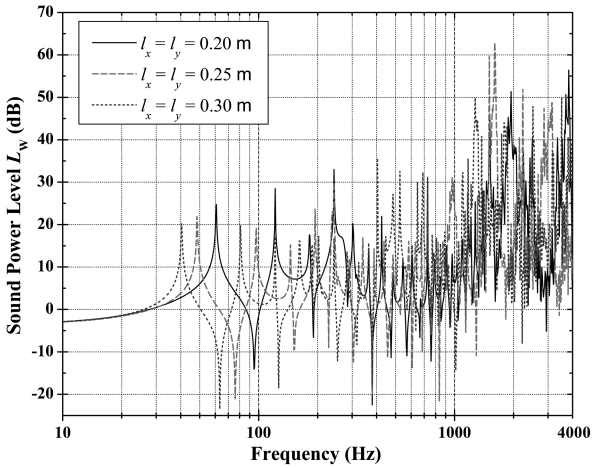

Fig. 6 Radiated sound power of the rib-stiffened plate (with reference to that of the bare plate) plotted as a function of frequency for various periodic spacings ($\varphi = 45$ deg, $\theta = 0$ deg, $M = 0.8$).

the midfrequency range. This happens because the sound impedance of the structure is dependent of the sound incidence angle: larger sound impedance associated with a higher incidence angle will noticeably reduce the sound radiation of the structure.

C. Effect of Periodic Spacings

As a key parameter of the rib-stiffened structures considered in this study, the spacing between two adjacent stiffeners in the x or y direction characterizes the periodicity of the structure. To explore the effect of structure periodicity on sound radiation, the radiated sound power is plotted in Fig. 6 as a function of frequency for several choices of periodic spacings, with $\varphi = 45$ deg, $\theta = 0$ deg, and $M = 0.8$. For simplicity, the stiffeners are taken as equally spaced along the x and y directions, $l_x = l_y$. As the periodic spacing is increased, whereas the whole tendency of the PWL versus frequency remains unchanged, the peaks and dips are noticeably shifted to lower frequencies (Fig. 6). This means that, for periodically rib-stiffened plates immersed in external mean flow, the natural frequencies of the plate decrease with increasing periodic spacings and relatively small alterations of the periodic spacings will not change broadly the periodicity nature of the structure. As the factual aircraft structures are often not perfectly periodic, the sound radiation behavior of locally nonperiodic structures is an interesting issue for aero-acoustical design of aircraft fuselages. This issue will be addressed in a separate study.

In the presence of mean flow, to gain more insights into the effect of periodic spacings on sound radiation, Fig. 7 plots the PWL of the

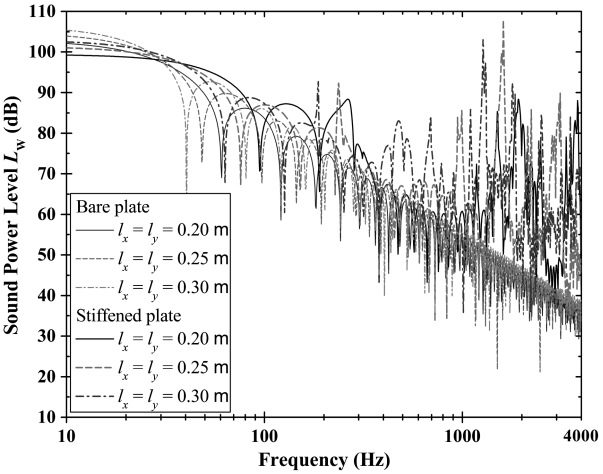

Fig. 7 Radiated sound power of the bare plate and the rib-stiffened plate (with reference to 10^{-12} W) plotted as a function of frequency for various periodic spacings ($\varphi = 45$ deg, $\theta = 0$ deg, $M = 0.8$).

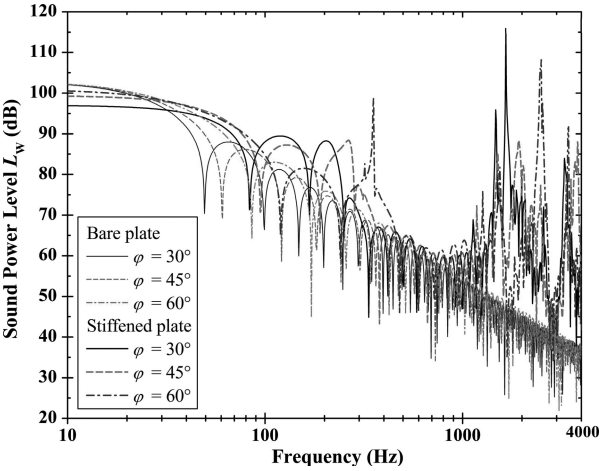

Fig. 5 Radiated sound power of the bare plate and the rib-stiffened plate (with reference to 10^{-12} W) plotted as a function of frequency for various incident angles ($\theta = 0$ deg, $M = 0.8$, $l_x = l_y = 0.2$ m).

rib-stiffened plate and the reference PWL of the bare plate for selected periodic spacings, with $M = 0.8$. As a reference, the sound power of the bare plate is calculated by a truncation manipulation [Eq. (37)] so that it has the same dimensions ($Ml_x \times Nl_y$) as the rib-stiffened plate, which is therefore also related to periodic spacings, as shown in Fig. 7. It is seen that the peaks and dips in the PWL versus frequency curves all move to lower frequencies as the periodic spacing is increased. Moreover, with increasing periodic spacing, the radiation sound power decreases in the low frequency range (<100 Hz) and increases in the high frequency range (<100 Hz) as far as the overall tendency is concerned. As a matter of fact, increasing the periodic spacing reduces the stiffness of the structure, which in turn causes the radiated sound power to decrease below 100 Hz and increase above 100 Hz.

IV. Conclusions

A theoretical model has been developed for sound radiation from aeroelastic plates stiffened by two sets of orthogonally distributed rib stiffeners and subjected to external jet noise, with particular focus placed upon the influence of the presence of convected mean flow. The model is built upon the Kirchhoff thin plate theory and the convected wave equation, with the Euler–Bernoulli bean equation and the torsional wave equation applied to describe the flexural and torsional motions of the rib stiffeners, respectively. In view of the periodic nature of the structure, the Poisson summation formula and the Fourier transformation technique are adopted to solve the

aeroelastic-acoustic governing equations of the system. To highlight the effects of external mean flow and structural periodicity, the sound pressure radiated by the structure is given in the form of a decibel scale with respect to that radiated by a bare plate immersed in stationary fluid.

To gain fundamental insights into the aeroelastic-acoustic behavior of rib-stiffened plates immersed in external mean flow, systematic numerical studies are carried out with the developed model to quantify the effects of mean flow speed, jet-noise incident angle, and stiffener spacings. It is established that the presence of mean flow significantly affects the sound radiation performance of the structure, dramatically reducing its PWL level at relatively low frequencies. As the mean flow Mach number is increased, whereas the location of the resonance peak on the PWL versus frequency curve remains nearly unchanged, the antiresonance dips move to higher frequencies. As the sound incidence angle is increased, the peaks and dips on the PWL curves are remarkably shifted to higher frequencies, leading to changes in the PWL value at specific frequencies and the resultant alteration of the whole curve tendency. As the periodic spacings are increased, the PWL peaks and dips all move to lower frequencies while the whole tendency of the curve remains unchanged.

The theoretical model presented in this study is capable of giving reasonable predictions for sound radiation of rib-stiffened aircraft fuselage structures, which is helpful for the evaluation of aircraft interior noise level at different cruise speeds and the design of aircraft skin structures at different locations with respect to the jet engine.

Acknowledgments

The authors appreciate the valuable suggestions from Dr. Steven Griffin and the equally valuable comments and great efforts from the anonymous reviewers. This work is supported by the National Basic Research Program of China (2011CB6103005), the National Natural Science Foundation of China (11102148, 11072188, and 11021202), and the Fundamental Research Funds for Central Universities (xjj2011005).

Appendix A: Derivation of Eq. (28)

The displacement components of the face plate in the wave number space are

$$\{U_{m'n'}\} = [\,U_{11}\quad U_{21}\quad \cdots\quad U_{M1}\quad U_{12}\quad U_{22}\quad \cdots\quad U_{M2}\quad \cdots\quad U_{MN}\,]^T_{MN\times 1} \tag{A1}$$

where

$$U_{m'n'} = \tilde{w}_1(\alpha'_m, \beta'_n) \tag{A2}$$

The right-hand side of Eq. (28) represents the generalized force:

$$\{Q_{m'n'}\} = [\,Q_{11}\quad Q_{21}\quad \cdots\quad Q_{M1}\quad Q_{12}\quad Q_{22}\quad \cdots\quad Q_{M2}\quad \cdots\quad Q_{MN}\,]^T_{MN\times 1} \tag{A3}$$

where

$$Q_{m'n'} = 2p_e\delta(\alpha'_m + \alpha_0)\delta(\beta'_n + \beta_0) \tag{A4}$$

$$\lambda_{1,m'n'} = D(\alpha'^2_m + \beta'^2_n)^2 - m\omega^2 - \omega^2\rho_0/\gamma_1(\alpha'_m, \beta'_n) - \omega^2\rho_0/\gamma_2(\alpha'_m, \beta'_n) \tag{A5}$$

$$T_1 = \begin{bmatrix} \lambda_{1,11} & & & & & & & & & \\ & \lambda_{1,21} & & & & & & & & \\ & & \ddots & & & & & & & \\ & & & \lambda_{1,M1} & & & & & & \\ & & & & \lambda_{1,12} & & & & & \\ & & & & & \lambda_{1,22} & & & & \\ & & & & & & \ddots & & & \\ & & & & & & & \lambda_{1,M2} & & \\ & & & & & & & & \ddots & \\ & & & & & & & & & \lambda_{1,MN} \end{bmatrix}_{MN\times MN} \tag{A6}$$

$$\lambda_{2,Mn'} = \frac{1}{l_x}\begin{bmatrix} (E_yI_y\beta'^4_n - m_y\omega^2) & (E_yI_y\beta'^4_n - m_y\omega^2) & \cdots & (E_yI_y\beta'^4_n - m_y\omega^2) \\ (E_yI_y\beta'^4_n - m_y\omega^2) & (E_yI_y\beta'^4_n - m_y\omega^2) & \cdots & (E_yI_y\beta'^4_n - m_y\omega^2) \\ \vdots & \vdots & \ddots & \vdots \\ (E_yI_y\beta'^4_n - m_y\omega^2) & (E_yI_y\beta'^4_n - m_y\omega^2) & \cdots & (E_yI_y\beta'^4_n - m_y\omega^2) \end{bmatrix}_{M\times N} \tag{A7}$$

$$T_2 = \begin{bmatrix} \lambda_{2,M1} & & & \\ & \lambda_{2,M2} & & \\ & & \ddots & \\ & & & \lambda_{2,MN} \end{bmatrix}_{MN\times MN} \tag{A8}$$

$$\lambda_{3,Mn'} = \frac{1}{l_x}(G_yJ_y\beta'^2_n - \rho_yI_{py}\omega^2)\begin{bmatrix} \alpha_1\alpha'_1 & \alpha_2\alpha'_1 & \cdots & \alpha_M\alpha'_1 \\ \alpha_1\alpha'_2 & \alpha_2\alpha'_2 & \cdots & \alpha_M\alpha'_2 \\ \vdots & \vdots & \ddots & \vdots \\ \alpha_1\alpha'_M & \alpha_2\alpha'_M & \cdots & \alpha_M\alpha'_M \end{bmatrix}_{M\times N} \tag{A9}$$

$$T_3 = \begin{bmatrix} \lambda_{3,M1} & & & \\ & \lambda_{3,M2} & & \\ & & \ddots & \\ & & & \lambda_{3,MN} \end{bmatrix}_{MN\times MN} \tag{A10}$$

$$\lambda_{4,MN} = \frac{1}{l_y}\begin{bmatrix} (E_xI_x\alpha_1'^4 - m_x\omega^2) & & & \\ & (E_xI_x\alpha_2'^4 - m_x\omega^2) & & \\ & & \ddots & \\ & & & (E_xI_x\alpha_M'^4 - m_x\omega^2) \end{bmatrix}_{M\times N} \tag{A11}$$

$$T_4 = \begin{bmatrix} \lambda_{4,MN} & \lambda_{4,MN} & \lambda_{4,MN} & \lambda_{4,MN} \\ \lambda_{4,MN} & \lambda_{4,MN} & \lambda_{4,MN} & \lambda_{4,MN} \\ \lambda_{4,MN} & \lambda_{4,MN} & \lambda_{4,MN} & \lambda_{4,MN} \\ \lambda_{4,MN} & \lambda_{4,MN} & \lambda_{4,MN} & \lambda_{4,MN} \end{bmatrix}_{MN\times MN} \tag{A12}$$

$$\lambda_{5,Mn',n} = \frac{1}{l_y}\beta_n'\beta_n \times \begin{bmatrix} (G_xJ_x\alpha_1'^2 - \rho_xI_{px}\omega^2) & & & \\ & (G_xJ_x\alpha_2'^2 - \rho_xI_{px}\omega^2) & & \\ & & \ddots & \\ & & & (G_xJ_x\alpha_M'^2 - \rho_xI_{px}\omega^2) \end{bmatrix}_{M\times N} \tag{A13}$$

$$T_5 = \begin{bmatrix} \lambda_{5,M1,1} & \lambda_{5,M1,2} & \cdots & \lambda_{5,M1,N} \\ \lambda_{5,M2,1} & \lambda_{5,M2,2} & \cdots & \lambda_{5,M2,N} \\ \vdots & \vdots & \ddots & \vdots \\ \lambda_{5,MN,1} & \lambda_{5,MN,2} & \cdots & \lambda_{5,MN,N} \end{bmatrix}_{MN\times MN} \tag{A14}$$

Employing the definition of the previously presented submatrices, one obtains

$$T = T_1 + T_2 + T_3 + T_4 + T_5 \tag{A15}$$

References

[1] Dowell, E. H., "Transmission of Noise from a Turbulent Boundary Layer Through a Flexible Plate into a Closed Cavity," *Journal of the Acoustical Society of America*, Vol. 46, No. 1B, 1969, pp. 238–252. doi:10.1121/1.1911676

[2] Koval, L. R., "Effect of Air Flow, Panel Curvature, and Internal Pressurization on Field-Incidence Transmission Loss," *Journal of the Acoustical Society of America*, Vol. 59, No. 6, 1976, pp. 1379–1385. doi:10.1121/1.381024

[3] Carneal, J. P., and Fuller, C. R., "Active Structural Acoustic Control of Noise Transmission Through Double Panel Systems," *AIAA Journal*, Vol. 33, No. 4, 1995, pp. 618–623. doi:10.2514/3.12623

[4] Frampton, K. D., Clark, R. L., and Dowell, E. H., "State-Space Modeling for Aeroelastic Panels with Linearized Potential Flow Aerodynamic Loading," *Journal of Aircraft*, Vol. 33, No. 4, 1996, pp. 816–822. doi:10.2514/3.47019

[5] Frampton, K. D., and Clark, R. L., "State-Space Modeling of Aerodynamic Forces on Plate Using Singular Value Decomposition," *AIAA Journal*, Vol. 34, No. 12, 1996, pp. 2627–2630. doi:10.2514/3.13449

[6] Atalla, N., and Nicolas, J., "A Formulation for Mean Flow Effects on Sound Radiation from Rectangular Baffled Plates with Arbitrary Boundary Conditions," *Journal of Vibration and Acoustics*, Vol. 117, No. 1, 1995, pp. 22–29. doi:10.1115/1.2873863

[7] Unruh, J. F., and Dobosz, S. A., "Fuselage Structural-Acoustic Modeling for Structure-Borne Interior Noise Transmission," *Journal of Vibration Acoustics Stress and Reliability in Design-Transactions of the ASME*, Vol. 110, No. 2, April 1988, pp. 226–233. doi:10.1115/1.3269503

[8] Mixson, J. S., and Roussos, L., "Laboratory Study of Add-on Treatments for Interior Noise Control in Light Aircraft," *Journal of Aircraft*, Vol. 20, No. 6, 1983, pp. 516–522. doi:10.2514/3.44902

[9] Xin, F. X., and Lu, T. J., "Analytical and Experimental Investigation on Transmission Loss of Clamped Double Panels: Implication of Boundary Effects," *Journal of the Acoustical Society of America*, Vol. 125, No. 3, March 2009, pp. 1506–1517. doi:10.1121/1.3075766

[10] Xin, F. X., Lu, T. J., and Chen, C. Q., "Vibroacoustic Behavior of Clamp Mounted Double-Panel Partition with Enclosure Air Cavity," *Journal of the Acoustical Society of America*, Vol. 124, No. 6, 2008, pp. 3604–3612. doi:10.1121/1.3006956

[11] Gardonio, P., and Elliott, S. J., "Active Control of Structure-Borne and Airborne Sound Transmission Through Double Panel," *Journal of Aircraft*, Vol. 36, No. 6, Nov.–Dec. 1999, pp. 1023–1032. doi:10.2514/2.2544

[12] Maury, C., Gardonio, P., and Elliott, S. J., "Model for Active Control of Flow-Induced Noise Transmitted Through Double Partitions," *AIAA Journal*, Vol. 40, No. 6, 2002, pp. 1113–1121. doi:10.2514/2.1760

[13] Alujevic, N., Frampton, K., and Gardonio, P., "Stability and Performance of a Smart Double Panel with Decentralized Active Dampers," *AIAA Journal*, Vol. 46, No. 7, 2008, pp. 1747–1756. doi:10.2514/1.34572

[14] Heitman, K. E., and Mixson, J. S., "Laboratory Study of Cabin Acoustic Treatments Installed in an Aircraft Fuselage," *Journal of Aircraft*, Vol. 23, No. 1, 1986, pp. 32–38. doi:10.2514/3.45263

[15] Frampton, K. D., and Clark, R. L., "Power Flow in an Aeroelastic Plate Backed by a Reverberant Cavity," *Journal of the Acoustical Society of America*, Vol. 102, No. 3, 1997, pp. 1620–1627. doi:10.1121/1.420073

[16] Clark, R. L., and Frampton, K. D., "Aeroelastic Structural Acoustic Coupling: Implications on the Control of Turbulent Boundary-Layer Noise Transmission," *Journal of the Acoustical Society of America*, Vol. 102, No. 3, Sept. 1997, pp. 1639–1647. doi:10.1121/1.420075

[17] Grosveld, F., "Plate Acceleration and Sound Transmission Due to Random Acoustic and Boundary-Layer Excitation," *AIAA Journal*, Vol. 30, No. 3, 1992, pp. 601–607. doi:10.2514/3.10962

[18] Xin, F. X., Lu, T. J., and Chen, C. Q., "Sound Transmission Through Simply Supported Finite Double-Panel Partitions with Enclosed Air Cavity," *Journal of Vibration and Acoustics*, Vol. 132, No. 1, 2010, pp. 011008-1–011008-11. doi:10.1115/1.4000466

[19] Xin, F. X., and Lu, T. J., "Analytical Modeling of Sound Transmission Through Clamped Triple-Panel Partition Separated by Enclosed Air Cavities," *European Journal of Mechanics – A/Solids*, Vol. 30, No. 6, 2011, pp. 770–782. doi:10.1016/j.euromechsol.2011.04.013

[20] Howe, M. S., and Shah, P. L., "Influence of Mean Flow on Boundary Layer Generated Interior Noise," *Journal of the Acoustical Society of America*, Vol. 99, No. 6, 1996, pp. 3401–3411. doi:10.1121/1.414988

[21] Maury, C., Gardonio, P., and Elliott, S. J., "Active Control of the Flow-Induced Noise Transmitted Through a Panel," *AIAA Journal*, Vol. 39, No. 10, Oct. 2001, pp. 1860–1867. doi:10.2514/2.1200

[22] Graham, W. R., "Boundary Layer Induced Noise in Aircraft, Part II: The Trimmed Plat Plate Model," *Journal of Sound and Vibration*, Vol. 192, No. 1, 1996, pp. 121–138. doi:10.1006/jsvi.1996.0179

[23] Mixson, J. S., and Powell, C. A., "Review of Recent Research on Interior Noise of Propeller Aircraft," *Journal of Aircraft*, Vol. 22, No. 11, 1985, pp. 931–949. doi:10.2514/3.45229

[24] Wilby, J. F., and Gloyna, F. L., "Vibration Measurements of an Airplane Fuselage Structure I. Turbulent Boundary Layer Excitation," *Journal of*

Sound and Vibration, Vol. 23, No. 4, 1972, pp. 443–466.
doi:10.1016/0022-460X(72)90503-2
[25] Wilby, J. F., and Gloyna, F. L., "Vibration Measurements of an Airplane Fuselage Structure II. Jet Noise Excitation," *Journal of Sound and Vibration*, Vol. 23, No. 4, 1972, pp. 467–486.
doi:10.1016/0022-460X(72)90504-4
[26] Gardonio, P., "Review of Active Techniques for Aerospace Vibro-Acoustic Control," *Journal of Aircraft*, Vol. 39, No. 2, March–April 2002, pp. 206–214.
doi:10.2514/2.2934
[27] Yeh, C., "Reflection and Transmission of Sound Waves by a Moving Fluid Laver," *Journal of the Acoustical Society of America*, Vol. 41, No. 4A, 1967, pp. 817–821.
doi:10.1121/1.1910411
[28] Ribner, H. S., "Reflection, Transmission, and Amplification of Sound by a Moving Medium," *Journal of the Acoustical Society of America*, Vol. 29, No. 4, 1957, pp. 435–441.
doi:10.1121/1.1908918
[29] Yeh, C., "A Further Note on the Reflection and Transmission of Sound Waves by a Moving Fluid Layer," *Journal of the Acoustical Society of America*, Vol. 43, No. 6, 1968, pp. 1454–1455.
doi:10.1121/1.1911012
[30] Xin, F. X., Lu, T. J., and Chen, C. Q., "External Mean Flow Influence on Noise Transmission Through Double-Leaf Aeroelastic Plates," *AIAA Journal*, Vol. 47, No. 8, 2009, pp. 1939–1951.
doi:10.2514/1.42426
[31] Sgard, F., Atalla, N., and Nicolas, J., "Coupled FEM-BEM Approach for Mean Flow Effects on Vibro-Acoustic Behavior of Planar Structures," *AIAA Journal*, Vol. 32, No. 12, 1994, pp. 2351–2358.
doi:10.2514/3.12299
[32] Wu, S. F., and Maestrello, L., "Responses of Finite Baffled Plate to Turbulent Flow Excitations," *AIAA Journal*, Vol. 33, No. 1, 1995, pp. 13–19.
doi:10.2514/3.12326
[33] Xin, F. X., and Lu, T. J., "Analytical Modeling of Sound Transmission Across Finite Aeroelastic Panels in Convected Fluids," *Journal of the Acoustical Society of America*, Vol. 128, No. 3, 2010, pp. 1097–1107.
doi:10.1121/1.3466861
[34] Legault, J., and Atalla, N., "Numerical and Experimental Investigation of the Effect of Structural Links on the Sound Transmission of a Lightweight Double Panel Structure," *Journal of Sound and Vibration*, Vol. 324, No. 3–5, 2009, pp. 712–732.
doi:10.1016/j.jsv.2009.02.019
[35] Legault, J., and Atalla, N., "Sound Transmission Through a Double Panel Structure Periodically Coupled with Vibration Insulators," *Journal of Sound and Vibration*, Vol. 329, No. 15, 2010, pp. 3082–3100.
doi:10.1016/j.jsv.2010.02.013
[36] Mejdi, A., and Atalla, N., "Dynamic and Acoustic Response of Bidirectionally Stiffened Plates with Eccentric Stiffeners Subject to Airborne and Structure-Borne Excitations," *Journal of Sound and Vibration*, Vol. 329, No. 21, 2010, pp. 4422–4439.
doi:10.1016/j.jsv.2010.04.007
[37] Frampton, K. D., and Clark, R. L., "Sound Transmission Through an Aeroelastic Plate into a Cavity," *AIAA Journal*, Vol. 35, No. 7, July 1997, pp. 1113–1118.
doi:10.2514/2.221
[38] Clark, R. L., and Frampton, K. D., "Aeroelastic Structural Acoustic Control," *Journal of the Acoustical Society of America*, Vol. 105, No. 2, Feb. 1999, pp. 743–754.
doi:10.1121/1.426265
[39] Frampton, K. D., "Radiation Efficiency of Convected Fluid-Loaded Plates," *Journal of the Acoustical Society of America*, Vol. 113, No. 5, 2003, pp. 2663–2673.
doi:10.1121/1.1559173
[40] Frampton, K. D., "The Effect of Flow-Induced Coupling on Sound Radiation from Convected Fluid Loaded Plates," *Journal of the Acoustical Society of America*, Vol. 117, No. 3, 2005, pp. 1129–1137.
doi:10.1121/1.1852894
[41] Schmidt, P. L., and Frampton, K. D., "Acoustic Radiation from a Simple Structure in Supersonic Flow," *Journal of Sound and Vibration*, Vol. 328, No. 3, 2009, pp. 243–258.
doi:10.1016/j.jsv.2009.08.005
[42] Alujevic, N., Gardonio, P., and Frampton, K. D., "Smart Double Panel with Decentralized Active Dampers for Sound Transmission Control," *AIAA Journal*, Vol. 46, No. 6, 2008, pp. 1463–1475.
doi:10.2514/1.32369
[43] Maestrello, L., "Responses of Finite Baffled Plate to Turbulent Flow Excitations," *AIAA Journal*, Vol. 33, No. 1, 1995, pp. 13–19.
doi:10.2514/3.12326
[44] Ingard, U., "Influence of Fluid Motion past a Plane Boundary on Sound Reflection, Absorption, and Transmission," *Journal of the Acoustical Society of America*, Vol. 31, No. 7, 1959, pp. 1035–1036.
doi:10.1121/1.1907805
[45] Kessissoglou, N. J., and Pan, J., "An Analytical Investigation of the Active Attenuation of the Plate Flexural Wave Transmission Through a Reinforcing Beam," *The Journal of the Acoustical Society of America*, Vol. 102, No. 6, 1997, pp. 3530–3541.
[46] Morse, P. M., and Ingard, K. U., *Theoretical Acoustics*, McGraw-Hill, New York, 1968, pp. 680–900.
[47] Xin, F. X., and Lu, T. J., "Analytical Modeling of Wave Propagation in Orthogonally Rib-Stiffened Sandwich Structures: Sound Radiation," *Computers and Structures*, Vol. 89, Nos. 5–6, 2011, pp. 507–516.
doi:10.1016/j.compstruc.2010.12.007
[48] Xin, F. X., and Lu, T. J., "Sound Radiation of Orthogonally Rib-Stiffened Sandwich Structures with Cavity Absorption," *Composites Science and Technology*, Vol. 70, No. 15, 2010, pp. 2198–2206.
doi:10.1016/j.compscitech.2010.09.001
[49] Xin, F. X., and Lu, T. J., "Analytical Modeling of Fluid Loaded Orthogonally Rib-Stiffened Sandwich Structures: Sound Transmission," *Journal of the Mechanics and Physics of Solids*, Vol. 58, No. 9, 2010, pp. 1374–1396.
doi:10.1016/j.jmps.2010.05.008
[50] Mace, B. R., "Sound Radiation from a Plate Reinforced by Two Sets of Parallel Stiffeners," *Journal of Sound and Vibration*, Vol. 71, No. 3, 1980, pp. 435–441.
doi:10.1016/0022-460X(80)90425-3
[51] Xin, F. X., and Lu, T. J., "Transmission Loss of Orthogonally Rib-Stiffened Double-Panel Structures with Cavity Absorption," *Journal of the Acoustical Society of America*, Vol. 129, No. 4, 2011, pp. 1919–1934.
doi:10.1121/1.3531947
[52] Rumerman, M. L., "Vibration and Wave Propagation in Ribbed Plates," *Journal of the Acoustical Society of America*, Vol. 57, No. 2, 1975, pp. 370–373.
doi:10.1121/1.380450
[53] Fahy, F., *Sound and Structural Vibration: Radiation, Transmission and Response*, Academic Press, London, 1985, pp. 135–240.
[54] Cunefare, K. A., "Effect of Modal Interaction on Sound Radiation from Vibrating Structures," *AIAA Journal*, Vol. 30, No. 12, Dec. 1992, pp. 2819–2828.
doi:10.2514/3.11624

S. Griffin
Associate Editor